FEATURE ARTICLE

Interfacial Rate Processes in Adhesion and Friction

Animangsu Ghatak, Katherine Vorvolakos, Hongquan She, David L. Malotky, and Manoj K. Chaudhury*

Department of Chemical Engineering, Lehigh University, Bethlehem, Pennsylvania 18015

Received: December 7, 1999; In Final Form: January 25, 2000

Adhesion between solid materials results from intermolecular interactions. The fracture resistance of an adhesive joint is, however, determined jointly by the mechanical deformation in the bulk material and the strength of the interfacial bond. The force needed to break an interfacial bond does not have a fixed value; it depends on the thermal state of the system and the rate at which the force is transmitted to the bond. The concomitant energy dissipation arising from the extension and the relaxation of the interfacial bonds contributes a significant resistance to fracture, which is clearly evident in elastomeric polymers. This issue of interfacial dissipation and its relationship to the length of the interfacial bridges and the rate of crack propagation are addressed with the kinetic theory of bond rupture in the tradition of the models developed by Eyring, Tobolsky, Zhurkov, Bueche, Schallamach, Kausch, and more recently, by Evans and Ritchie. Next, the method is extended to address the velocity-dependent sliding friction of elastomers against low energy solid surfaces. The theme of this article is to point out that certain aspects of adhesion, friction, and fracture may be described under a generalized framework of interfacial kinetics.

1. Introduction

Most interfacial processes are rate dependent, suggesting that they are coupled to energy dissipative processes occurring either in the bulk or at the interface of the materials. Examples of rate-dependent processes include fracture of an adhesive interface, friction between surfaces, and the dynamic wetting of liquids on solid surfaces.

Although the rate-dependent interfacial processes play key roles in various macroscopic phenomena, they do not always come to light, as conventional wisdom often dictates that interfacial processes are thermodynamically reversible. Take the case of fracture in solids as an example. According to Griffith,[1] the externally applied energy, which is stored elastically in a material, is ultimately used up to propagate a crack. The reduction of the elastic energy, which is balanced exactly by the energy gained in the creation of two new surfaces, is recovered when the crack closes again. Griffith's criterion applies rather well to low energy elastic materials and when a crack moves at an extremely slow speed. Usually, the energy needed to fracture an interface is larger than the thermodynamic free energy of adhesion, meaning that some energy is dissipated.[2−4] A classic way to tackle the problem is to treat the fracture as a process, in which the dissipation in the bulk is proportional to a reversible free energy of adhesion. Although such a treatment may appear to be useful in decoupling the bulk and interfacial processes, the fundamental assumption of bulk irreversibility being coupled to the interfacial reversibility in a multiplicative way requires further examination. A somewhat similar situation arises in the dynamics of wetting or dewetting of liquids on solid surfaces. Here, the verdict of classical continuum mechanics,[5−7] namely, that the shear stress is infinity at the liquid−solid contact line, poses a great difficulty for a liquid to spread on a solid surface. The fact that liquid spreads means that the singular shear stress is relaxed at the contact line, presumably by a molecular kinetic process.[8] In wetting, as in fracture, it remains to be understood how the bulk viscous processes are coupled to the kinetic processes at the contact line region.

Significant efforts have been made in the past decade toward finding a common connection among such seemingly unrelated phenomena as wetting, friction, and fracture.[9] The basis of these studies is the structure−property correlation with well-defined model systems. An experimental system which is quite friendly to this purpose is poly(dimethylsiloxane). The polymer is available in the form of a liquid, and is easily cross-linked to an elastomeric network. It has a glass transition temperature of −120 °C, meaning that the segmental motion of a PDMS-based elastomer is like that of a liquid at room temperature.[10,11] The polymer interacts weakly with other materials; but it is amenable to covalent bonding if required. Upon exposure to an oxygen plasma, the surface of the polymer readily converts to a silica-like structure (Figure 1), which can be used as a support for self-assembled alkylsiloxane monolayers.[12,13] With little ingenuity, the polymer can be molded to various shapes and forms, which poses fascinating prospects for various types of mechanical and interfacial studies.

The soft elastic property of the polymer makes it ideally suited for the method of contact mechanics,[14] in which a hemispherical object is brought into contact with another flat or hemispherical object under controlled loads. As soon as the two objects touch each other, a circular deformation develops in the zone of contact, which further increases with external load. From a

---

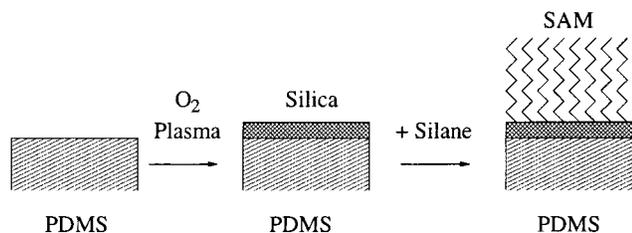* Author to whom correspondence should be addressed.

Feature Article

J. Phys. Chem. B, Vol. 104, No. 17, 2000 **4019**

Figure 1. Schematics of a method[12] used to form self-assembled alkylsiloxane monolayers (SAM) on PDMS elastomer. An oxygen plasma generates a thin silica-like surface on the elastomer, which is reacted with alkyl or perfluoroalkyl-trichlorosilanes to form the mono-layers.
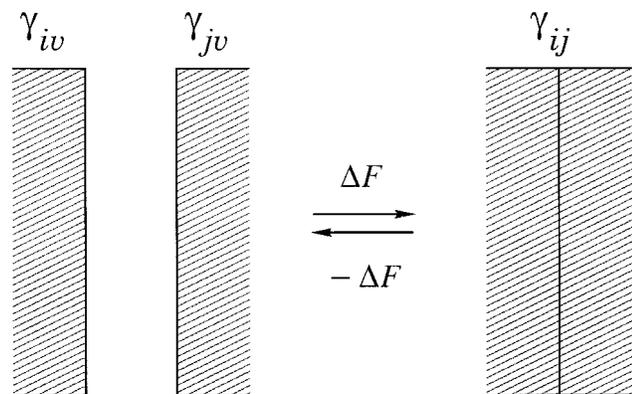

Figure 2. Thermodynamically reversible adhesion and fracture of two materials.

mechanical calibration of the deformation as a function of applied load, the interaction between various materials can be accurately estimated. A variant of this method is to slide the hemisphere laterally,[15] which allows measurement of the interfacial shear stress. Thus, equipped with a simple yet versatile method of mechanics, and empowered with various surface synthetic strategies, systematic investigations in wetting, adhesion, and friction have been possible in recent years. The results of some of these ongoing studies, particularly those related to the adhesion and frictional behavior of elastomeric polymers, are described in the subsequent sections. The article is organized as follows. We start our discussion by introducing some elementary concepts of adhesion and fracture and the methods used to measure adhesion energy at solid−solid interfaces. Next, we introduce the kinetic theory of bond breaking in order to explain certain rate and molecular weight dependent fracture behaviors of polymeric interfaces. Subsequently, we examine the rate-dependent processes of polymeric friction at solid−solid and solid−liquid interfaces. The article ends by highlighting some unsolved issues in adhesion and friction.

2. Fundamental Concepts of Adhesion and Fracture

Adhesion between two surfaces is established by intermolecular forces. Quantitatively, it is expressed in terms of the change of the Helmholtz free energy in the process of joining two surfaces[16] (Figure 2):

$$\Delta F = \gamma_{ij} - \gamma_{iv} - \gamma_{jv} \tag{1}$$

where v stands for vapor, γ_{ij}, γ_{iv}, and γ_{jv} are the interfacial and surface free energies of the ij, iv, and jv interfaces, respectively. ΔF, which is equivalent to the work of adhesion W, usually varies between 40 and 200 mJ/m² when the predominant force across an interface is dispersion, polar, hydrogen bonding, or

acid−base interaction. It is on the order 1−2 J/m² when an interface is held by covalent forces.

The energy (ΔF) needed to fracture an interface is derived from the mechanically stored strain energy in the material. If U_p, U_E, and U_s denote the potential, elastic, and surface energies, then the crack propagation criterion in an energy conservative system is[17] where A stands for the area of the interface. Equation

$$-\frac{d}{dA}(U_p + U_E) = \frac{dU_s}{dA} \tag{2}$$

2, which is the Griffith's criterion of fracture, implies that the strain energy release rate [$G = -(d/dA)(U_P + U_E)$] per unit extension of the crack area is equal to the thermodynamic work of adhesion ($W = dU_s/dA$) in a reversible situation. When $G > W$, the excess energy (also known as a crack driving force) has to be dissipated in a sustained fashion, i.e.,

$$(G - W)V = T\dot{S} \tag{3}$$

where $\dot{S}$ is the rate of entropy production at or near the crack tip region. In order to interpret the processes occurring at interfaces, it is important that the values of both G and W be determined separately and unambiguously. Below, we describe the methods of contact mechanics in order to accomplish this objective.

3. Contact Mechanics

When a hemispherical solid substrate comes into contact with another hemispherical or flat object, the adhesion forces acting across the interface tend to deform the solids and thus increase their area of contact. At equilibrium, the elastic forces are balanced by the interfacial forces with the following result:[14,18]

$$G = \frac{\left(\dfrac{4E^*a^3}{3R} - P\right)^2}{8\pi E^* a^3} \tag{4}$$

where P is the external force applied on the hemisphere of radius R, and a is the radius of contact. E^* is given by $1/E^* = (1 - v_1^2)/E_1 + (1 - v_2^2)/E_2$; v and E being the Poisson's ratio and elastic modulus, respectively. At its simplest level, the experimental methodology involves bringing a deformable hemispherical object into contact with a flat substrate under controlled loads (Figure 3). When the hemisphere touches the flat substrate, a circular deformation develops in the contact zone, which increases with external load (Figure 4). After the load reaches a certain value, it is then decreased and the contact deformation is measured until the two materials separate. Mechanical calibration of these load-deformation data using eq 4 yields the strain energy release rate G. Usually, two values of G are obtained (Figure 4): one from the loading (i.e., crack closure) and the other from the unloading (i.e., crack opening) branch of the load-deformation cycle.[9,19] These two adhesion energies can also be determined by another version of contact mechanics, which is based on the rolling of a hemicylinder or hemisphere on a flat substrate.[20−25] As the hemicylinder or hemisphere rolls, a crack opens at the trailing edge while another crack closes at the leading edge of contact. Measurements of the rolling torque and the contact width allow simultaneous estimation of the strain energy release rates (G) corresponding to the crack opening and closing processes. When any of the above two studies is carried out with elastic materials, the strain energy release rate (G) obtained from the crack closure corresponds closely to the thermodynamic work of adhesion W, whereas that obtained from
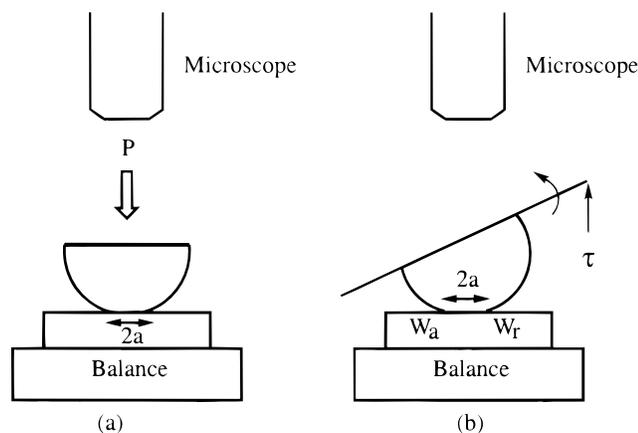
Figure 3. Schematics of the methods of contact mechanics used to measure adhesion energies at solid−solid interfaces. In (a), a hemispherical solid is pressed against a flat surface under a controlled load (P). The load deformation data in conjunction with eq 4 yield the adhesion energy between the two surfaces. In (b) a hemispherical object is rolled on a flat surface. Here the rolling torque (τ) and the contact widths are needed to estimate the adhesion energies at leading (W_a) and trailing (W_r) edges, respectively.
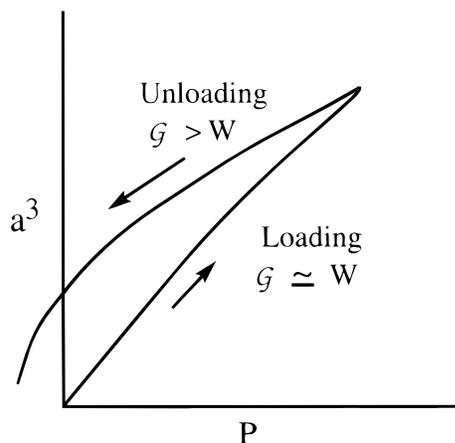

Figure 4. Typical load deformation behavior obtained from the JKR contact mechanics experiment.

the crack opening is greater than W. The excess energy ($\mathcal{G} - W$) carries signatures of the nonequilibrium processes occurring in the materials.

4. Previous Findings

Careful studies by Barquins and Maugis[26,27] clarified that the viscoelastic deformation in the bulk of the materials and the concomitant energy dissipation can be significant contributors to the irreversibility seen with many contact mechanics studies. An empirical equation to account for the energy dissipation was proposed earlier by Gent and Schultz,[2] as well as by Andrews and Kinloch:[3]

$$\mathcal{G} - W = W\phi(a_T V) \qquad (5)$$

where ϕ is a dimensionless viscoelastic dissipation function that depends on the viscoelastic properties of the materials, the crack speed V, and temperature T; a_T is the Williams−Landel−Ferry (WLF) shift factor.

The experimental adhesion energy ($\mathcal{G}$) usually varies with crack velocity following a power law with the exponent ranging from 0.1 to 0.5. Kendall,[28] in an attempt to discern the
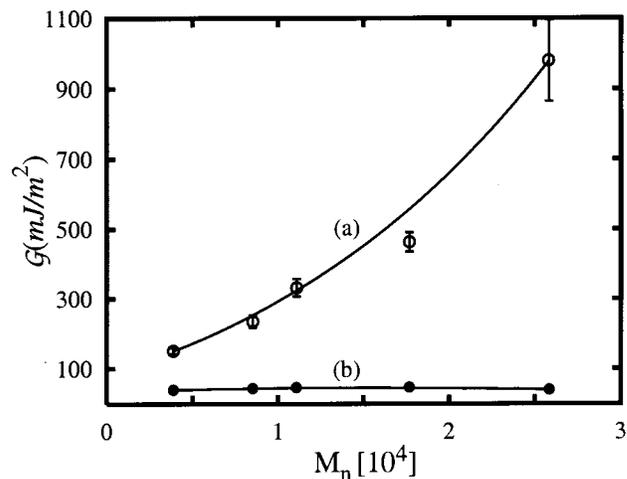

Figure 5. Dependence of the fracture energy on the molecular weight of polymers (see also Figure 7). (a) Represents the H-bonding interaction of PDMS and silica. (b) represents the dispersion interaction of PDMS with hexadecylsiloxane-coated silica.

contributions of the interfacial and the bulk viscoelastic drag in fracture, noticed that the interfacial kinetic processes contribute significantly to adhesion hysteresis. Kendall's findings, which were significant departures from previously held beliefs, led to the possibility that a crack may be arrested by the kinetic processes ocurring right at the interface. These findings, however, required further support from experiments in whichthe interfacial kinetic processes could be studied independently of the viscoelastic processes.

Several studies carried out in recent years have focused the issue even further. Chaudhury and Whitesides[12,13] combined a surface modification strategy with JKR contact mechanics to probe into the role of interfacial chemistry in adhesion hysteresis. Poly(dimethylsiloxane), modified with self-assembled organic monolayers, formed the basis for these studies. It was observed that silicone elastomers, coated with hydrocarbon monolayers, exhibit negligible hysteresis in the contact mechanics experiments, whereas those coated with fluorocarbon monolayers exhibit significant hysteresis. A more interesting case is the contact of hydrocarbon and fluorocarbon monolayers, in which the hysteresis exhibits a time-dependent response. It was stipulated that multiple metastable states exist at the interface of real materials. When the energy barriers separating the metastable states are significantly larger than the characteristic vibrational and thermal energies of the system, the interface does not relax within any experimentally observable time frame. On the other hand, when the energy barriers are comparable to thermal and vibrational energies, the contact area exhibits a time-dependent relaxation with a concomitant dissipation of strain energy. These studies provided support to Kendall's supposition quite convincingly that significant drag to crack propagation can arise from rate-dependent processes occurring right at the interface. Further support to the idea of interfacial dissipation was gathered from a study by Shanahan and Michel,[29] who noticed that adhesion hysteresis between a styrene−butadiene hemisphere and glass increases with the inter-cross-link molecular weight of the rubber. A follow up to these studies was carried out by us, in which we noticed significant molecular weight dependent adhesion hysteresis between poly(dimethylsiloxane) and silica[24] (Figure 5a). The molecular weight dependent hysteresis, however, disappeared completely when the silica was rendered non-hydrogen bonding by coating it with a self-assembled hydrocarbon monolayer (Figure 5b). Additional
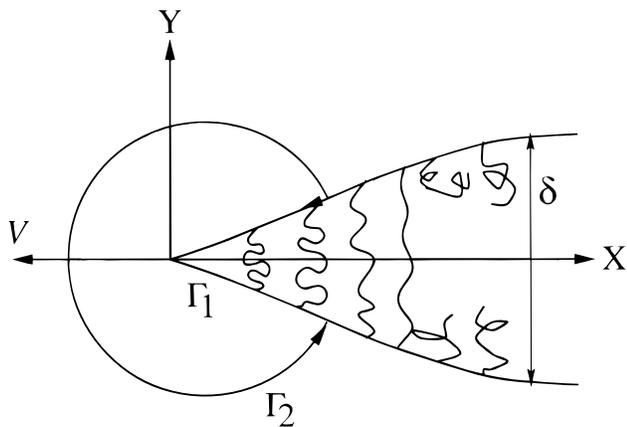
Feature Article

J. Phys. Chem. B, Vol. 104, No. 17, 2000 **4021**

Figure 6. Figure 6. A crack bridged by polymer chains is moving left with a velocity V.

results, to be presented in section 6, point out that when an H-bonding or covalent interaction dominates the interfacial adhesion, the fracture energy exhibits a weak velocity dependence,[30] whereas no significant velocity dependence is seen with an interface dominated by dispersion forces. Answers to some of these observations can be found in what is known as the Lake–Thomas effect.[31]

5. Lake–Thomas Effect

The molecular weight dependence of the fracture resistance of polymeric interfaces was first discovered by Lake and Thomas[31] while studying the tear properties of rubbers. Based on the typical number of chains ($10^{18}/m^2$) that cross a fracture plane and the energy needed (400 kJ/mol) to break a single chemical bond, the total energy of fracture of an elastomeric rubber should be only about $1-2$ J/m^2. Experimental values of fracture energies, however, range from 10 to 100 J/m^2. Lake and Thomas provided a remarkable insight into the problem by noting that the polymer chains at and in the vicinity of the crack are highly stretched. When one of the bonds breaks, the chain relaxes at zero load and thus all of the stored elastic energy is dissipated. Since all the bonds in the chain must be activated to their breaking points before only one bond breaks, the energy dissipation is proportional to the number of bonds in a polymer chain. The molecular fracture energy ($1-2$ J/m^2), thus amplified by the number of bonds in a chain, comes close to what is observed ($10-100$ J/m^2) experimentally. The argument can be understood by using Barenblatt's cohesive zone model[32] and Rice's J-integral[33] method of evaluating the energy release rate. Rice introduced an integral (J) defined as

$$J = \int_\Gamma \left(\epsilon dy - \vec{T} \frac{\partial \vec{u}}{\partial x} ds \right) \quad (6)$$

where ϵ is the strain energy density, Γ is a curve surrounding the crack tip, $\vec{T}$ is the traction vector, $\vec{u}$ is the displacement vector, and ds is an element of arc length along Γ. Γ can be any path surrounding the crack from its upper surface to lower surface in a counterclockwise direction (Figure 6). Rice demonstrated that the value of J is path independent; i.e., $J_{\Gamma_1} = J_{\Gamma_2}$, which immediately leads to Griffith's criterion of fracture. Evaluation of J along the path Γ_2 yields the elastic strain energy release rate G. However, when the path Γ_1 is chosen, J becomes the interfacial energy release rate:

$$J = \int_{\Gamma_1} \vec{T} \frac{\partial \vec{u}}{\partial x} ds = \int_{\delta_0}^{\infty} \sigma(\delta) \, d\delta \quad (7)$$

where $\sigma(\delta)$ is the restraining stress between the open surfaces of the crack.

When a crack closes, van der Waals interactions provide the only force at the interface. Thus, $\sigma(\delta) = A/(6\pi\delta^3)$, A being the Hamaker constant. The J integral then becomes equal to $A/(12\pi\delta_0^2)$—the usual van der Waals work of adhesion W. When the crack opens in a polymer, the restraining stress is contributed by the elastic tension in the bridging zone, and eq 7 becomes

$$G = J = \Sigma_o \int_{\delta_0}^{\delta_{max}} k_s \delta \, d\delta + W = \Sigma_o \frac{k_s \delta_{max}^2}{2} + W \quad (8)$$

where Σ_o is the areal density of the bridging polymer and k_s is its spring constant. In eq 8, $k_s\delta_{max}^2/2$ is equivalent to nU and $\Sigma_o \propto n^{-1/2}$, where n is the number of bonds per chain and U is the energy stored in a bond before the chain dissociates. G thus becomes

$$G - W \simeq \Sigma_o nU \propto n^{1/2}U \quad (9)$$

Equation 9 is the classical Lake–Thomas result,[31,34] showing that the fracture energy is amplified by the number of bonds in a chain. Although this theory explains why the fracture energy increases with molecular weight, it does not explain why it is rate dependent and why the effect is dependent on the types of interaction prevailing across an interface. These issues are addressed next, after emphasizing a few important points.

First, we note that the derivation of eq 9 is based on the assumption that a bond breaks at a fixed force. This assumption, as pointed out by Evans and Ritchie,[37] is correct only at absolute zero temperature. At a finite temperature, energy states are thermalized and bond breaking events follow stochastic[35–38] paths. When the thermal state of a bond is near the high energy tail of the Maxwellian energy distribution, it dissociates spontaneously. However, the bonds that are initially at the ground energy state, need to cross the energy barrier by thermal activation. Several authors,[35–48] following Eyring's[49] lead, recognized the significance of the kinetic bond dissociation in adhesion and friction. The subject was reviewed nicely by Kausch[48] and is elaborated upon in the next section.

6. Thermally Activated Bond Dissociation and Fracture

According to Eyring, a force F applied to a chemical bond modifies the activation energy of the bond dissociation by $-F\lambda$, where λ is the activation length of the bond. When an interface is subjected to a stress, the number of chains bridging the two surfaces decreases according to the following equation:[50]

$$-\frac{D\Sigma_b}{Dt} = \tau_-^{-1} n\Sigma_b \exp\left(\frac{F\lambda}{kT}\right) - K_+\Sigma_u \quad (10)$$

where Σ_b and Σ_u are the areal densities of the polymer chains in the bonded and nonbonded states, respectively, and K_+ is the rate constant of bond association. The relaxation time (τ_-) of bond dissociation may be expressed as follows:

$$\tau_- = \left(\frac{h}{kT}\right) \exp\left(\frac{E_a}{kT}\right) \quad (11)$$

where E_a is the activation energy of bond dissociation and h is Plank's constant. The factor n in eq 10 implies that any of the bonds in the polymer chain can dissociate. We assume that a polymer chain in the cohesive zone behaves like a linear spring, with a spring constant k_s. Since the force ($F = k_s\delta$) on the bond increases with the chain extension δ, the rate of bond cleavage

can be described by the following nonlinear equation: Σ_0 (=

$$-\frac{D\Sigma_b}{Dt} = \tau_-^{-1}\Sigma_b n \exp\left(\frac{k_s\delta\lambda}{kT}\right) - K_+(\Sigma_0 - \Sigma_b) \quad (12)$$

$\Sigma_b + \Sigma_u$) is the total number of chains per unit area. The rate of bond association is usually much smaller than the rate of bond dissociation, and thus can be neglected in the kinetic crack growth situations.[50] To an observer moving with the crack, the areal distribution of polymer chains in the bridging zone would be described as follows:

$$-\alpha V\frac{d\Sigma_b}{d\delta} = \frac{1}{\tau_-}\Sigma_b n \exp\left(\frac{k_s\delta\lambda}{kT}\right) \quad (13)$$

Here $\alpha = d\delta/dx$ is the slope of the crack face, which, for simplicity, is taken to be a constant. The average extension of the polymer chain can be expressed as follows:

$$\bar{\delta} = \int_0^\infty \frac{\Sigma_b}{\Sigma_0} d\delta \quad (14)$$

Once δ is estimated from eqs 13 and 14, the average force on a chain before it breaks into two parts can be expressed as $F = k_s\bar{\delta}$. The solutions of eqs 13 and 14 can be expressed as the following exponential integral function:[39,50]

$$\bar{\delta} = \left(\frac{kT}{k_s\lambda}\right)\exp\left(\frac{nkT}{k_sV\lambda\tau_-\alpha}\right)\int_{\frac{nkT}{k_sV\lambda\tau_-\alpha}}^\infty q^{-1}\exp(-q)\,dq \quad (15)$$

Another level of simplification of eq 15 is possible when $nkT \ll k_sV\lambda\tau_-\alpha$. In that case, the exponential integral function becomes

$$\bar{\delta} \simeq \left(\frac{kT}{k_s\lambda}\right)\left[\ln\left(\frac{k_sV\lambda\tau_-\alpha}{nkT}\right)\right] \quad (16)$$

The average force ($k_s\bar{\delta}$) on a chain thus varies logarithmically with the crack velocity, which is similar to the conclusion reached by Evans et al.[37,38] Once the average force to dissociate a bond is known, the total fracture energy can be calculated as follows:

$$\mathcal{G}_{el} = \int_0^{F_m}\Sigma_b F\,d\delta = \left(\frac{\Sigma_0}{2k_s}\right)\left[\left(\frac{kT}{\lambda}\right)\ln\left(\frac{k_sV\lambda\tau_-\alpha}{nkT}\right)\right]^2 \quad (17)$$

The spring constant (k_s) of a polymer is inversely proportional to the number of monomers (n) in the chain, whereas $\Sigma_0 \sim n^{-1/2}$. We thus have from eq 17, $\mathcal{G}_{el} \sim n^{1/2}$—the classical Lake—Thomas result ($\mathcal{G} \sim n^{1/2}U$). However, the bond dissociation energy U of the Lake—Thomas theory is now replaced with a function that contains kinetic parameters. The classical Lake—Thomas effect, i.e., the molecular weight dependent amplification of the fracture energy, can be understood on the basis of the nonequilibrium aspect of the bond dissociation phenomenon. Close to thermodynamic equilibrium, however, there is no Lake—Thomas amplification of fracture energy as there is no energy dissipation.[50] Equation 17 reveals numerous characteristics of polymer fracture in terms of its dependence on the molecular weight (n) of the bridging polymer, the rate of crack propagation (V), and the interfacial chemistry via the relaxation time τ_-. Here the relaxation time is important, because fracture energy can be virtually independent of the molecular weight if τ_- is very small. This is exactly what is observed when interfacial interaction is primarily due to dispersive forces
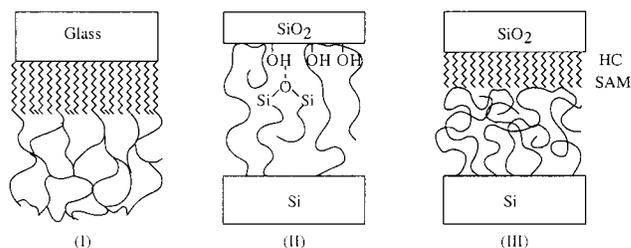

Figure 7. Three model systems used for fracture studies (see also Figure 1). Case I involves covalent bonding of a silicone elastomer to glass via a coupling agent. Case II involves the H-bonding interaction between plasma-oxidized PDMS and thin films of poly(dimethylsiloxane)s grafted onto a silicone wafer. In case III, the plasma-oxidized PDMS is pre-reacted with hexadecylsiloxane (HDS) and then is contacted with a PDMS film. The HDS-modified surface interacts with the PDMS films only by dispersion forces.
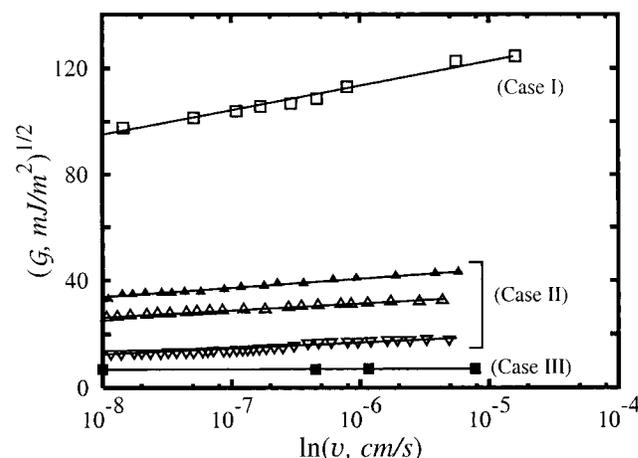

Figure 8. Fracture energy increases logarithmically with the rate of crack propagation except when the dispersion forces dominate the interfacial interaction. Three types of adhesive interfaces are studied here. Case I ($\square$) corresponds to a covalent interaction between glass and a silicone elastomer. In this case, significant chain scission occurs at the glass—polymer interface. Case II corresponds to H-bonding interaction between silica and end-tethered silicone polymers of various molecular weights. $\blacktriangle$, $\triangle$, and $\triangledown$ correspond to the molecular weights of 25.8 kD, 17.7 kD, and 3.8 kD, respectively. Case III ($\blacksquare$) corresponds to the dispersion interaction between a silicone elastomer and a hexadecylsiloxane monolayer adsorbed on silica.

(Figure 5b) for which the relaxation time is on the order of a microsecond or less. Numerical calculations show that the average extensions ($\bar{\delta}$) of the chains are negligible for such fast relaxations and thus the only contribution to fracture energy comes from the long-range dispersion forces ($A/12\pi\delta_o^2$) between the open surfaces of the crack.

Molecular weight dependent fracture in the case of H-bonding interaction (Figure 5a) implies that the relaxation of bond dissociation is relatively slow. In order to obtain rough estimates of these relaxation times, we have carried out fracture experiments at various crack growth rates according to the methods described in refs 24 and 50. For the purpose of comparison, three types of interactions are considered (Figure 7). The first case involves a covalent bonding between a PDMS rubber and a glass. The second case involves the H-bonding interaction between PDMS and silica, whereas the third case involves only dispersion interactions. Figure 8 shows that the fracture energies, in all these cases, vary logarithmically with the velocity of crack opening ($v = \alpha V$), except when the surfaces interact via dispersion interaction. These observations are roughly consistent with eq 17 in the following form:

Feature Article

J. Phys. Chem. B, Vol. 104, No. 17, 2000 **4023**

$$\sqrt{G} = \left(\sqrt{\frac{\Sigma_0}{2k_s}}\right)\left(\frac{kT}{\lambda}\right)\ln(v) + \sqrt{\frac{\Sigma_0}{2k_s}}\left(\frac{kT}{\lambda}\right)\ln\left(\frac{k_s\lambda\tau_-}{nkT}\right) \quad (18)$$

where we have removed the subscript in G, and $v(= \alpha V)$ is the velocity of crack opening in the direction perpendicular to the crack growth. In view of eq 18, the relaxation time (τ_-) of bond dissociation can be obtained from the slopes and intercepts of the lines in Figure 8. Note that n in eq 18 is equal to unity when the polymer chains desorb from the surface without any chain scission. The lack of any significant velocity dependence of the fracture energy for the dispersion interaction confirms that the relaxation of the interfacial bond is very fast. Later in this article, in connection with the kinetic theory of rubber friction, we show that τ_- is on the order of 1 μs for surfaces interacting with dispersion forces. By contrast, τ_- for the breaking of polymer chains (case I) is about 10^{13} s. For H-bonding interactions, τ_- varies from 10^4 s for a molecular weight of 3.7 kD to 10^{10} s for a molecular weight of 26 kD. This increase of the bond relaxation time as a function of molecular weight implies that the polymer chains do not desorb cleanly from the silica surface and that some scission of polymer chains occurs during interfacial separation when the molecular weight is high. This implication is consistent with the earlier observations of She et al.[24,51]

The activation energy of the siloxane bond scission (case I) estimated from its relaxation time ($\sim 10^{13}$ s), is 151 kJ/mol, which is considerably smaller than the dissociation energy (454 kJ/mol) of a siloxane bond. The discrepancy arises due to several over-simplified assumptions that were used in deriving eq 17. First, we note that the transition state theory (TST) of Eyring is based on the assumption that the transition state and ground state are in thermal equilibrium. The rate of escape over the barrier is obtained by multiplying the equilibrium density of states near the barrier with the frequency of a thermal photon (kT/h). The correct way to calculate the rate, as was shown by Kramers,[52,53] is by considering the fact that the bonds at ground energy state cross the energy barrier by a diffusion process either in the spatial or in the energy coordinate. Kramers' formalism leads to a different expression for the transition probability than that predicted by the TST model. Secondly, the assumption of a transition state having a fixed transition length is flawed. As demonstrated clearly by Kausch[47] and Evans et al.,[37,38] the transition state itself is modified by the force. As an example, let us consider that the interaction between two atoms is described by a Morse potential, upon which a mechanical potential is superimposed (Figure 9).

We need to calculate the rate at which a state at A crosses that at B. The transition rate[53] is approximated as follows:

$$k(f) = \left[\frac{2\pi\omega_2(f)}{\omega_1(f)\left(\sqrt{\frac{\eta^2}{4} + (2\pi\omega_2(f))^2} - \frac{\eta}{2}\right)} + \frac{kT}{\eta E_a(f)}\right]^{-1} \times$$
$$\exp\left(-\frac{E_a(f)}{kT}\right) \quad (19)$$

Here $\omega_1(f)$ and $\omega_2(f)$ are the frequencies in the parabolic approximation of the energy potentials in the ground and transition states, respectively. $E_a(f)$ is the activation energy, and η measures the friction (or the rate of the Maxwellian velocity relaxation) of the molecular bonds. When η is large, eq 19 assumes the Smoluchowski limit,[56] in which a bond dissociates spatially due to Brownian impact, as is the case[37,38] with many biological complexes in liquid water. In the breaking of a
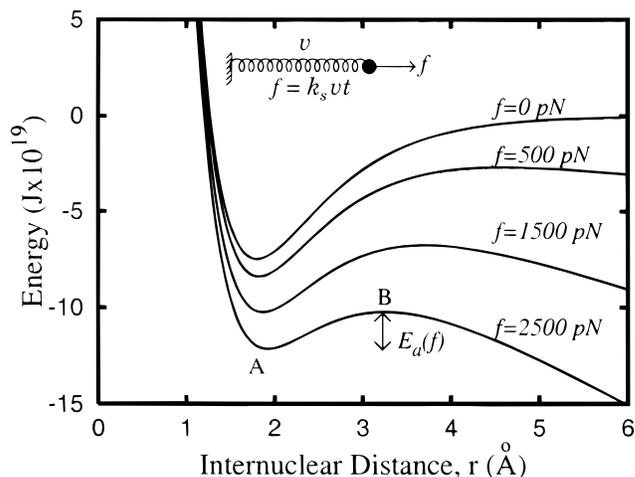

Figure 9. A test Morse potential for a SiO bond modified by various mechanical potentials. The resultant potential is of the form $V = (f^2/2k_s) + V_{Morse} - fr$, where f is the force applied to a bond with a spring of spring constant k_s and r is the internuclear distance. In this model, the ground state of zero energy is defined for the spring in the relaxed state. Since we are interested in the relative shapes of the potentials at different values of f, we have plotted $V_{Morse} - fr$ as a function of r. The depth of the potential at zero force is 454 kJ/mol. Its frequency at the ground state is 2×10^{13} s^{-1}. Note that both the activation energy and the activation length decreases with increasing force.

covalent bond, however, η must be contributed by the relaxations of internal states. The effect of friction (η) on the force needed to break a polymer chain can be found by solving eq 20 in conjunction with eq 19:

$$-k_s v \frac{d\phi}{df} = nk(f)\phi \quad (20)$$

where ϕ is the fraction of the total number of polymer chains that survive after a time t and $f = k_s vt$, where k_s is the spring constant of the polymer chain (Figure 11) and v is the velocity at which the chain is stretched. Numerical solution of eq 20 shows that ϕ remains nearly constant as force increases and then drops to zero catastrophically beyond a critical force. The critical force needed to break a bond varies nearly parabolically with η, the minimum value of which approaches the TST estimate (Figure 10). We do not have a clear picture of the magnitude of η in a polymer chain; it should be related to the damping of bond vibrations. A rough estimate of η/ω_1 is $\sim 1/50$, which predicts that the bond breaking force is close to that predicted by the TST model. The inset of Figure 10 shows that the force to break a bond increases logarithmically with velocity. If these data are forced to fit Schallamach's model as described by eq 16, the needed values of λ and E_a are 1 Å and 216 kJ/mol, respectively. Note that the activation energy of this forced fit is much smaller than the actual depth (454 kJ/mol) of the Morse potential, which is similar to our experimental observations. It thus appears that even though the TST model may not be a bad approximation to calculate the bond dissociation force, a fixed value of the transition length λ can lead to serious error. For the sake of simplicity we will continue to use the TST model in the rest of this article. However, we take note of the fact that both the transition length λ and the activation energy (E_a) are adjustable parameters within this model.

The effect of relaxation time on adhesion raises an interesting issue about how the fracture energy in a viscoelastic system is coupled to the interfacial processes. The standard methods e.g., those of Gent and Schultz[2] and of Andrews and Kinloch,[3] lump all the energy dissipation to the bulk viscoelastic processes while
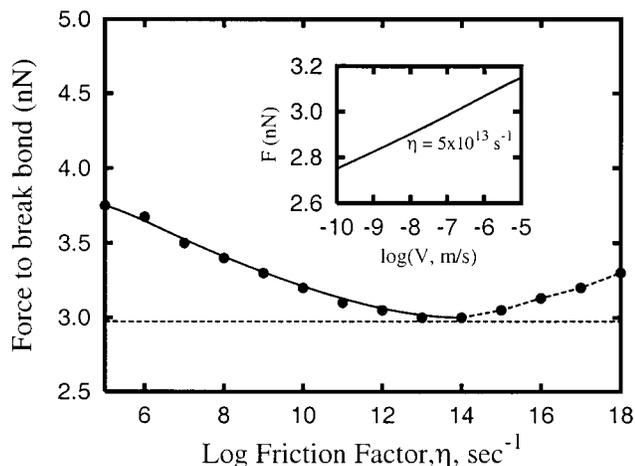
Figure 10. The force needed to break a bond depends on the friction η (see eq 20). Here the bond is connected to a polymer chain of spring constant ~ 0.6 N/m, the typical spring constant of a PDMS chain obtained from AFM measurements (see Figure 11). These calculations were done at $V = 10^{-7}$ m/s. The inset shows that the force to break a bond increases logarithmically with the velocity of stretching the polymer chain.

Figure 11. Extensile behaviors of tethered PDMS chains studied using an atomic force microscope (AFM[54]). Data obtained from independent measurements are superimposed by plotting the force against the fractional extension of the polymer. The arrows indicated the forces at which the different chains detached from the tip. The normalization was guided by a persistence chain model[55] of rubber elasticity (solid line) with a persistence length of 0.15 nm. The theoretical model agreed with experimental data up to a chain extension of 90% of the contour length L_c. The average spring constant of the polymer in the region of high extension is $\sim 27/L_c$, where L_c is in nm.

assuming the interface to separate reversibly. Total fracture energy is expressed as a product of the thermodynamic work of adhesion (W) and a bulk viscoelastic function (ϕ) as shown in eq 5. The kinetic theory of bond failure, however, precludes reversible separation of an interface at reasonable crack growth rates, except in the case of a purely dispersive interaction, where a quasi-equilibrium behavior prevails. However, when an interface equilibrates much faster than the bulk, there is simply not enough time for the bulk viscoelastic drag to take effect at the crack tip. The interfacial drag must delay the crack opening in order to allow time for deformation and dissipation to be effective in the bulk of the adhesive. A possible mechanism by which the interfacial and bulk viscous processes are coupled may be shown with a simple example, in which a surface-adsorbed polymer chain is connected to a viscous dash-pot. Under the action of constant viscous force, chains desorb from the surface according to the following equation:

$$-\frac{d\Sigma_b}{dt} = \frac{\Sigma_b}{\tau_-} \exp\left(\frac{\mu V \lambda}{kT}\right) \qquad (21)$$

where μ is the viscous friction coefficient. The solution of eq 21 is exponential in t from which the average bond survival time is of the form: $\bar{t} = \tau_- \exp(-\mu V \lambda/kT)$. The energy dissipation corresponding to the detachment of a chain now shows a strong velocity dependence:

$$\varepsilon = \mu V^2 \tau_- \exp(-\mu V \lambda/kT) \qquad (22)$$

Re-examination of the fracture behavior of viscoelastic materials is of considerable importance in pressure-sensitive adhesive industry, particularly in controlling the release properties of an adhesive.[57-60] A purely van der Waals surface of low relaxation time is desirable in order to achieve extremely low release force. The fracture energy can be enhanced by introducing only very small amounts of H-bonding functional groups, which increase the interfacial relaxation time without altering surface energy in a significant way (Figure 12).

Coupling of a surface to a viscoelastic adhesive may have two consequences. Since the molecular bonds are connected to a medium of high viscosity, the bond dissociation rate constant,
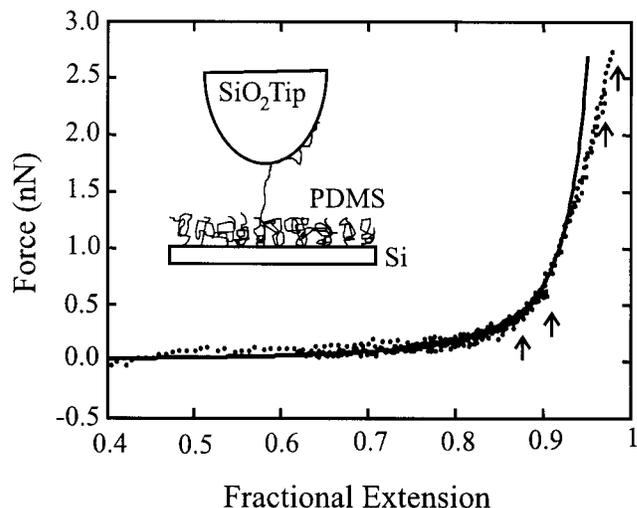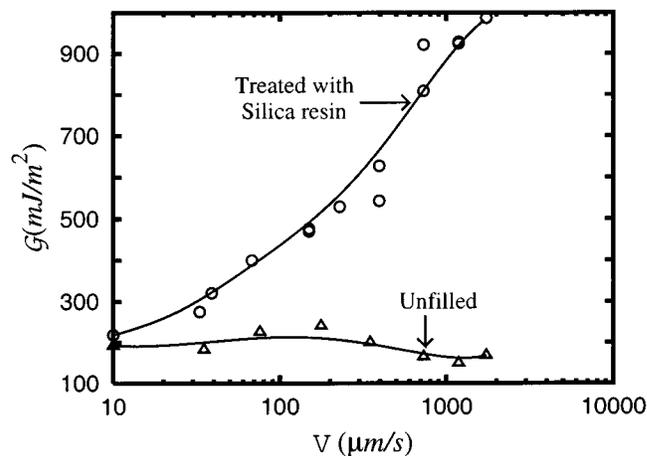

Figure 12. Fracture energy of silicone elastomers against an acrylic pressure-sensitive adhesive obtained using rolling contact mechanics. Note that the fracture energy of the unfilled rubber shows negligible velocity dependence suggesting that the bulk viscoelastic processes are not sufficiently coupled to the interface. Silica resin modified polymer can form weak H-bonds with the PSA, in which bulk viscoelasticity is coupled significantly to the interface as evident from the stronger velocity dependence of fracture energy.

according to Kramers' model, itself decreases. The other consequence is that the bond survival time is high because a constant viscous force acts on the bond as opposed to the case of a purely elastic system. A complete theory of viscoelastic fracture in terms of the interfacial and bulk kinetic processes still remains to be solved.

7. Activated Rate Theory of Rubber Friction

Our discussion, so far, has focused on one type of interfacial separation, in which the molecular bonds are broken perpendicular to the direction of crack propagation. We now turn our attention to another type of interfacial separation in which the surfaces slide past each other. In this second case, numerous

Feature Article

J. Phys. Chem. B, Vol. 104, No. 17, 2000 **4025**

bonds break even as the interface is displaced by the length of only one bond. Sliding friction is, therefore, a highly energy dissipative process and is not yet well understood.[61] Some of the challenging questions in this field are summarized below:

1. Do the surfaces slide past each other by collective motions of molecules, or is the sliding mediated by the propagation of dislocations?[9,62-64]

2. Do the collective motions of molecules or those of dislocations depend on the size of contact?[65,66]

3. What are the interfacial modes of energy dissipation in frictional sliding, and how do those modes interact with the overall system dynamics?

Considerable amounts of work are currently being conducted in different fields of physics, chemistry, and engineering to address the above questions. The subject is very broad and is beyond the scope of this article. Here, we focus on the frictional behavior of elastomeric polymers as the discussion is relevant to our previous topics dedicated to understanding elastomeric adhesion.

Systematic study of friction in polymeric systems was first carried out by Grosch,[67] who noted that the friction at a rubber–glass interface depends strongly on velocity and temperature. On the basis of Grosch's observations, Schallamach[39] developed an adhesion-based theory of rubber friction and proposed the molecular kinetic theory of polymer chain desorption. Schallamach considered that a polymer chain can exist either in the relaxed or in the surface bound state. If t_0 and $\bar{t}$ are the average times spent by the polymer chain in the unbound and the surface-bound states, then the fraction of chains in the bound state is $\bar{t}/(\bar{t} + t_0)$. Total interfacial stress supported by the polymer chains can therefore be expressed as

$$\sigma = k_s V \bar{t} \left[\frac{\Sigma_0 \bar{t}}{(\bar{t} + t_0)} \right] \qquad (23)$$

where k_s and Σ_o are the spring constant and the areal density of the polymer chains respectively; V is the sliding velocity. Equation 23 captures two effects: one is that the force on a polymer chain increases with velocity, and the other is that the number of chains in contact with the surface decreases with velocity. Interfacial shear stress therefore passes through a maximum value, as was observed by Grosch. Recently, Semenov et al.[68,69] considered the frictional behavior of polymers confined in narrow spaces. An important aspect of their analysis is similar to that of Schallamach, in which the number of contacts between the polymer and substrate changes with sliding velocity.

We investigated the frictional behavior of silicone elastomers of various inter-cross-link molecular weights on three low energy non-H-bonding surfaces: polystyrene and self-assembled monolayers of alkyl and perfluoroalkyl siloxanes. Friction was measured using a method of Brown[70] and Chaudhury[71,72] by mounting a hemispherical PDMS lens on one end of a spring (Figure 13), the other end of which is rigidly fixed. The substrate, against which friction is measured, is first broughtinto contact with the lens on a microscope stage. When the substrate is given a sudden displacement, the lens, at first, moves with it. Subsequently, the lens is dragged on the substrate as the spring wire continues to recover its neutral position. From the deflection of the spring wire as a function of time, sliding velocity is determined. The interfacial shear stress is calculated by dividing the spring force with the area of contact (Figure 13). The frictional results of a silicone elastomer having an inter-cross-link molecular weight of 3.5 K on the three low energy
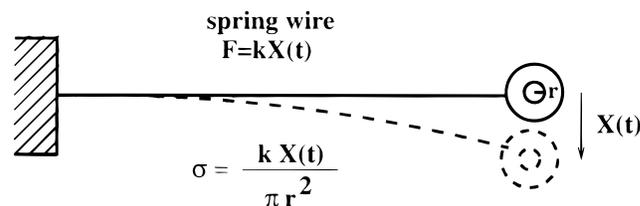

Figure 13. Schematics of the method used to measure the friction of a silicone rubber against a solid substrate. The lens is dragged on the surface as the spring recovers its neutral position. The friction force is calculated by knowing the spring constant (73 N/m) and the deflection $X(t)$. This force divided by the area of contact yields the shear stress.
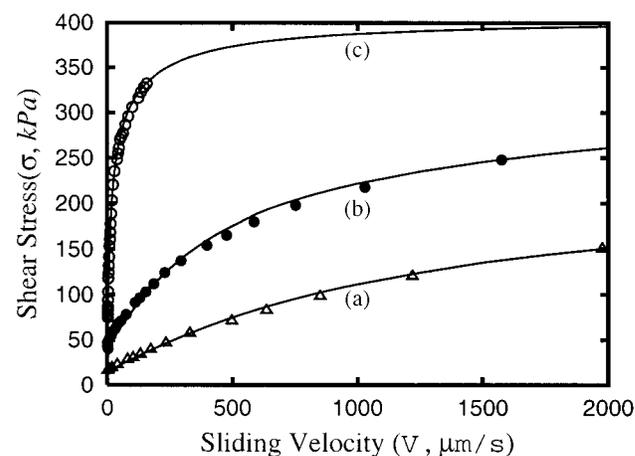

Figure 14. Shear stress of a PDMS elastomer on three low-energy surfaces. (a) and (b) indicate self-assembled monolayers of fluorocarbon ($O_{3/2}Si(CH_2)_2(CF_2)_7CF_3$) and hydrocarbon ($O_{3/2}Si(CH_2)_{15}CH_3$) on silicon wafer and (c) denotes polystyrene, respectively. Friction on polystyrene could not be measured at velocities higher than 200 μm/s, because of the occurrence of instabilities. The solid lines are obtained from eq 27 and 29 by adjusting the values of Σ_o and τ. PDMS elastomers used for these studies were produced by cross-linking vinyl-ended dimethyl-siloxanes (3.5 K) via platinum-catalyzed hydrosilation.

surfaces are summarized in Figure 14. It is remarkable that the friction force of PDMS on polystyrene is significantly higher than those on the fluorocarbon and hydrocarbon surfaces, even though the adhesion energy of PDMS on polystyrene (~45 mJ/m²), as measured by the method of contact mechanics, differ only slightly from those on the hydrocarbon (~42 mJ/m²) and fluorocarbon (~34 mJ/m²) surfaces. Another important fact is that the areas of contact between the PDMS lenses and the substrates remain constant at all sliding speeds, implying perhaps that adhesion does not change during sliding. Earlier, Brown had made similar observations.[70] We try to understand these results using the method of Schallamach, with an important difference. Schallamach[39] considered only two states: bound and relaxed. A two-state model is however incomplete, as a surface presents a multitude of energy traps to a polymer chain. Our picture of elastomeric sliding is as follows. We consider that the interface between the polymer and the substrate is composed of Σ_0 numbers of polymeric springs. One end of each spring is fixed to the polymer network, whereas the other end undergoes a biased random walk on the surface by hopping from one potential well to the next (Figure 15). We estimate the probability $p(x)$ of finding a chain in a particular stretched condition by solving a dynamic probability[73] balance equation as follows:

$$\frac{\mathrm{D}p(x)}{\mathrm{D}t} = [J_{(x+\lambda)\to x} + J_{(x-\lambda)\to x} - J_{x\to(x+\lambda)} - J_{x\to(x-\lambda)}] \qquad (24)$$

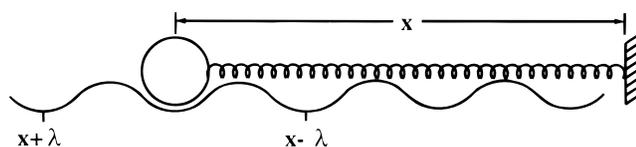**4026** *J. Phys. Chem. B, Vol. 104, No. 17, 2000*

Feature Article

Figure 15. Schematic of the method used to calculate friction force. One end of the polymer chain is fixed whereas the other end undergoes biased random walk on a surface by hopping from one potential well to the next. Random walk is possible in both positive and negative x, the maximum value of which cannot exceed the contour length of the polymer chain (L_c), i.e., $-L_c < x < L_c$. The fixed end moves with the reference frame at velocity V.

where $J_{i \to j}$ indicates the rate at which the polymer segment jumps from site i to j. The operation D/Dt implies a differential operation in time and space: D/D$t = \partial/\partial t + V(\partial/\partial x)$. $J_{i \to j}$ can be expressed as

$$J_{i \to j} = \frac{p_i}{2\tau} \exp\left(\pm \frac{f(x)\lambda}{2kT}\right) \qquad (25)$$

where p_i is the occupancy in the ith state and $f(x)$ is the force acting on the chain end corresponding to a chain extension x. The positive and negative signs in eq 25 signify jumps toward the right or left directions respectively in Figure 15. λ ($\sim$4 Å) is the characteristic lattice length. $p(x \pm \lambda)$ can be estimated from $p(x)$ by Taylor series expansion:

$$p(x \pm \lambda) = p(x) \pm \left(\frac{\partial p}{\partial x}\right)\lambda + \frac{\lambda^2}{2}\frac{\partial^2 p}{\partial x^2} \pm \dots \qquad (26)$$

Using the definitions in eqs 25 and eq 26 for other terms, eq 24 can be written as

$$\frac{\partial p}{\partial t} + V\frac{\partial p}{\partial x} = \frac{\lambda}{\tau}\sinh\left(\frac{f\lambda}{2kT}\right)\frac{\partial p}{\partial x} + \frac{\lambda^2}{2\tau}\cosh\left(\frac{f\lambda}{2kT}\right)\frac{\partial^2 p}{\partial x^2} \qquad (27)$$

Equation 27 readily converts to the well-known Smoluchowski equation of diffusion in a gravitational field in the limit of $f(x) << kT/\lambda$. To solve eq 27, we take the force on the entropic elastic spring to follow a persistence chain model:[55]

$$f = \frac{kT}{A}\left[\frac{1}{4}\left(1 - \frac{x}{L_c}\right)^{-2} - \frac{1}{4} + \frac{x}{L_c}\right] \qquad (28)$$

where L_c and A ($\sim$3.8 Å) are the contour and persistence lengths of the PDMS chain. We solve the steady-state version of eq 27 to find out the probability distribution of the extension of the polymer chain at different sliding velocities. The frictional stress at the interface (σ) is estimated using the following equation:

$$\sigma = \frac{\Sigma_o \int_{-L_c}^{L_c} p(x)\, f(x)\, \mathrm{d}x}{\int_{-L_c}^{L_c} p(x)\, \mathrm{d}x} \qquad (29)$$

Equations 24−29, however, do not account for a small but finite frictional stress observed experimentally at zero shear velocity. Without knowing its origin, we have tentatively added an empirical static shear stress to shift the baseline of the dynamic shear stress calculated using eqs 28 and 29. The values of Σ_o and τ needed to fit the experimental data in Figure 14 are 1.5 $\times$ 10^{16} m^{-2} and 0.38 μs for the fluorocarbon surface, 1.8 $\times$ 10^{16} m^{-2} and 1 μs for the hydrocarbon surface, and 2.0 $\times$ 10^{16} m^{-2} and 27 μs for polystyrene, respectively. The areal chain densities turn out to be remarkably close to each other for all

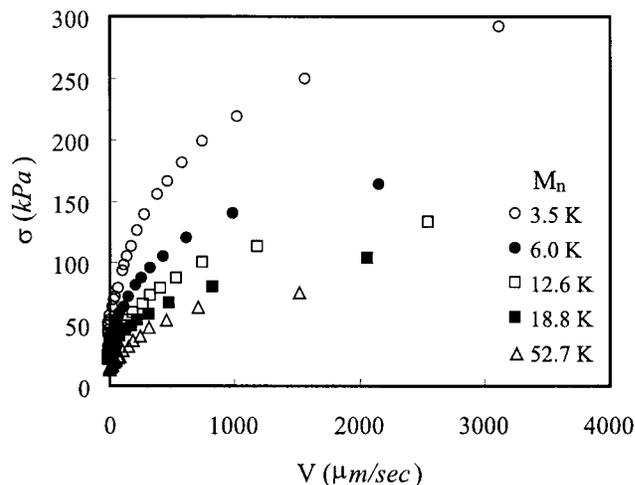**Figure 16.** Shear stress (σ) at the interface of a self-assembled monolayer of n-hexadecylsiloxane (O$_{3/2}$Si(CH$_2$)$_{15}$CH$_3$ and PDMS elastomer of various molecular weights. The inter-cross-link molecular weights of the elastomers are shown in the inset.

three surfaces, whereas the segmental relaxation times differ considerably. The longer relaxation time on polystyrene is consistent with the loss of chain mobility conjectured earlier by Brown.[70] However, the rigidity of the surface contributing to the loss of mobility, as proposed earlier, is probably of secondary consequence. The answer lies primarily in the difference in the interaction forces, however small it may be. Since the segmental relaxation time varies with the activation energy exponentially, $\tau \sim \exp(E_a/kT)$, a small change in the latter quantity could affect friction in a dramatic way. Assuming the validity of the transition state theory, the activation energies of PDMS on three surfaces are estimated as follows: 45 kJ/mol on polystyrene, 38 kJ/mol on hydrocarbon, and 35 kJ/mol on fluorocarbon surfaces. These energies are considerably higher than the typical depths of van der Waals potentials (3−5 kJ/mol), perhaps implying that clusters of several segments of dimethylsiloxane move in a correlated fashion on a surface. However, those energies adjusted by the areal chain densities (Σ_o) of the idealized polymer springs, amount to adhesion energies (1.0−1.5 mJ/m^2) which are in clear disagreement with those (35−45 mJ/m^2) obtained from the direct contact mechanics methods. There are no clear answers to these discrepancies. The results might, however, imply that friction measures the interaction of segments that are in direct physical contact, which is smaller than the mean field interaction of the two surfaces as probed by contact mechanics. There are, however, other factors to consider: for example, the change of the cohesive energy of the chains during the unfolding process.

An important finding of these studies is that the elastomeric friction, in contrast to adhesion, at first decreases with the increase of the inter-cross-link molecular weight (Figure 16) of the network, but then seems to reach a limiting value at high molecular weights ($\geqslant$ 18 K g/mol). Numerical calculations show that the force needed to slide a polymer chain on a surface is nearly independent of its molecular weight. Hence, the molecular weight dependent frictional stress is probably related to the effective areal density of the polymer chain, which, at first, decreases with the increase of the molecular weight of the polymer, but seems to reach a constant value at high molecular weights.

The interfacial shear stress between PDMS and polystyrene, as calculated using eq 29, varies weakly with the sliding speed, when $V > 200 \mu$m/s. Experimentally, it was difficult to probe

Feature Article

J. Phys. Chem. B, Vol. 104, No. 17, 2000 **4027**

this region due to the occurrence of stick−jump type instabilities at these sliding speeds. Recently, Casoli et al.[74] explored successfully the frictional behavior of a PDMS elastomer on various surfaces up to a sliding speed of 10 cm/s. They report two distinct behaviors: the first is a nearly velocity-independent friction on high energy surfaces such as silicon wafer, and the second is a (logarithmic) velocity-dependent friction on low energy surfaces. These differences, reflecting the differences in the segmental relaxation times, are qualitatively consistent with our observations.

Our simple model does not account for many details of interfacial interactions that prevail on real surfaces. One important factor is the nano- or microscale level surface corrugations that could affect the surface diffusion of the polymer chain and thus friction. The model also does not account for the cooperative dynamics of the polymeric segments on a surface presenting multiple meta-stable states, which is particularly important when the energy barriers separating these meta-stable states are comparable to the mechanical potential energy (i.e., at small forces). The collective Brownian motion of polymer chains, in that case, may either be completely frustrated or so slow that one may be misled to believing that a true static friction exists.

Because of space limitations, we are not able to touch upon another important subject that deals with the differences of the frictional behavior of the fluorocarbon and hydrocarbon surfaces and their relationships to adhesion hysteresis.[63] These discrepancies are brought about by a number of factors, including the structural differences and the triboelectric charging that occur so spontaneously on the fluorocarbon surfaces. We also noted that the frictional behavior of a pure PDMS network, as used in the current studies, are quite different from those of silica-filled commercial elastomers to the extent that a fluorocarbon SAM exhibits higher friction than a hydrocarbon SAM. The frictional behaviors of the fluorocarbon and hydrocarbon SAMs also depend strongly on the chain length, the packing density, and the substrates that support them. These topics will be discussed in detail separately.

8. Slippage of Polymer Melt on Low Energy Surface

A problem of considerable significance to polymer processing is the slip[75−86] behavior of the melt on solid surfaces. It is thought that the often-observed shark-skin-like patterns on the surface of injection molded polymers are due to the flow instabilities associated with slippage. It had been suspected for a long time that the hydrodynamic no-slip boundary condition at the wall may be violated by the entangled polymer melts.[77] Now it has been proven experimentally that, depending on the interactions of the polymeric melt with the solid surface and the applied shear stress, two types of slip behavior could be observed.[75] When the interaction is strong and the hydrodynamic stress is weak, interfacial chains disentangle from the bulk polymer leading to what is known as the apparent wall slip. Conversely, on a weakly interacting surface the polymer melt undergoes infinite slippage. The existences of apparent and true slips have been demonstrated by Léger et al.[75] in an experiment involving the flow of a high molecular weight ($M_w \sim 970\,000$) polymer (PDMS) melt on a low energy hydrocarbon surface. True slip occurred at the interface when the hydrodynamic shear stress exceeded 35 kPa, below which only apparent slip was observed. Interestingly, the shear stress vs slip velocity data obtained from these experiments fall in the same range as those obtained from our experiments on elastomeric friction on similar low energy solid surfaces. This observation is important for a
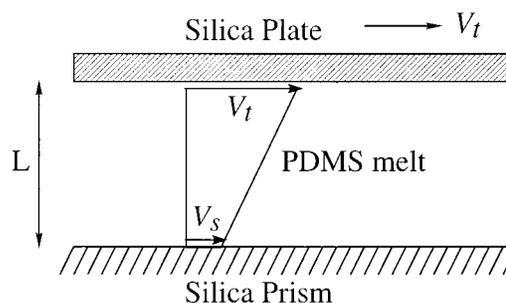

Figure 17. Schematic of the method used by Léger et al. to measure slip of a high molecular weight (970 000) PDMS melt on a octadecyl-silane-treated silica prism. The shear stress on the lower surface was produced by moving the top plate at a velocity V_t. Slippage of polymer was investigated using an evanescent wave method that probes the interface within a length scale of 1000 Å.
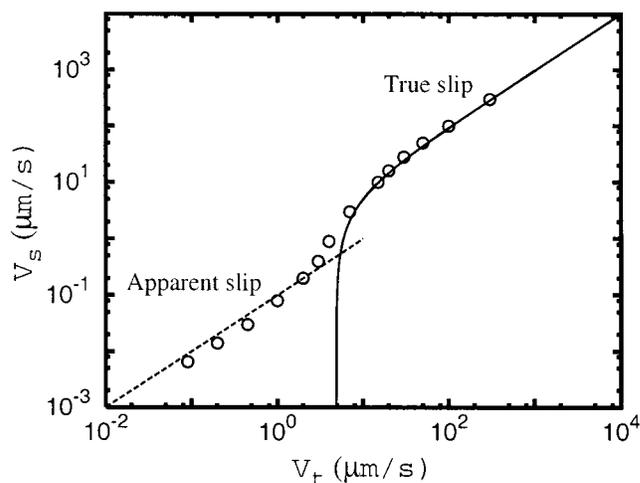

Figure 18. Slip velocity at the interface between PDMS polymer and hydrophobic glass as a function of the top plate velocity in the experiment of Léger et al. The solid line is the prediction of the slip velocities based on rubber friction data.

number of reasons. First, it supports our previous finding that the frictional stress reduces to a limiting value when the molecular weight is very high. Second, it indicates that molecular mechanism of friction at solid−solid or solid−liquid interfaces are not different at high sliding speeds. We therefore proceeded further to correlate the data obtained from these two entirely different experiments.

Assuming a linear velocity profile between the two plates in the experiment of Léger et al. (Figure 17), the interfacial shear stress in the fluid can be written as $\sigma = \mu(V_t - V_s/L)$. If we take the shear stress to be the same as the interfacial shear stress obtained from the rubber friction experiments in the limit of high inter-cross-link molecular weight, we can estimate how V_s should depend on V_t. Figure 18 compares the V_t vs V_s data obtained from the experiment of Léger et al. and those obtained from this analysis. The two slip regimes are very evident in the experimental data. In the true slip regime, the data agree very well with those obtained from our analysis. Interestingly, the theoretically predicted slip velocity becomes zero when the top plate velocity is less than a critical value ($\sim$5.0 μm/s). Experimentally, this is where the transition from the true to apparent slip occurs.

9. Mixed Mode Fracture

The discussion so far dealt with two distinct types of interfacial separation. In the first case, the interface opens
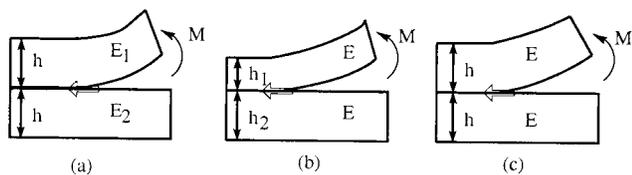
Figure 19. Shear stress develops at the interface in any of these asymmetric cases. The shear stress can be relieved by a slip process near the crack tip. *M* is the moment of a force acting on the crack.
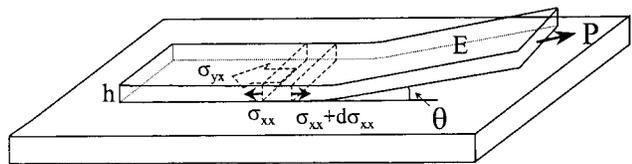

Figure 20. Sketch of an elastic ribbon peeling from a surface at a very low angle (θ). A thin section of the rubber experiences an elastic tensile stress (σ_{xx}) and an interfacial shear stress (σ_{yx}). The force balance on a differential cross section of the ribbon gives the equation for slip displacement (see eq 31−35).

perpendicular to crack propagation, and, in the second case, surfaces slide past each other. Fracture at real interfaces usually involves a mixed mode, resulting from some sort of asymmetry arising from the differences in geometry or from the mismatch of elastic properties of the materials[87] (Figure 19). In these cases, cracks just cannot open up and propagate without one material shearing against the other. The shear stress, thus developed, concentrates and diverges at the crack tip. Since the crack tip cannot support an infinite shear stress, some amount of interfacial sliding, either by slippage or by the emissions of dislocations, occurs at the crack tip. The crack driving force ($G − W$) is thus used up in overcoming the frictional processes at and near the crack tip regions:

$$(G − W)V = \int_0^\infty \sigma(v)\, v\, \mathrm{d}x \tag{30}$$

The power dissipation due to interfacial sliding can be evaluated if we know how the shear stress $\sigma(v)$ varies with slip velocity v and how it varies along the interface.[72,88] These points can be illustrated with the example of a thin elastomer film peeling from a surface.[72] Figure 20 shows a thin cross section of the elastomer in contact with a low energy substrate. When a tensile force is applied to the film, the strip tends to stretch, while interfacial friction prevents it. The balance of forces on a thin cross section of the film yields the following equation:

$$\frac{\partial \sigma_{xx}}{\partial x} = \frac{\sigma_{yx}}{h} \tag{31}$$

where σ_{xx} and σ_{yx} are the normal and shear stresses, respectively. σ_{xx} is related to the slip displacement u and elastic modulus of the film according to the following equation:

$$\sigma_{xx} = E\frac{\partial u}{\partial x} \tag{32}$$

The shear stress σ_{yx} varies with the interfacial slip velocity, v, in a nonlinear way as shown in Figure 16. For calculational comfort, we describe the $\sigma \sim v$ relationship with a power law equation:

$$\sigma_{yx} = \sigma_o + kv^n \tag{33}$$

By curve fitting the $\sigma \sim v$ data, the value of n is usually found

to be approximately 1/3. Under steady-state peeling, the slip velocity v is related to the crack velocity (V) as follows:

$$v = \mathrm{V}\frac{\partial u}{\partial x} \tag{34}$$

Equations 31−34 now can be combined to yield the following equation:

$$\frac{\mathrm{d}^2 u}{\mathrm{d}x^2} = \frac{\sigma_o}{Eh} + \frac{kV^n}{Eh}\left(\frac{\mathrm{d}u}{\mathrm{d}x}\right)^n \tag{35}$$

Solution of eq 35 yields the slip displacement (u) of the elastomer as a function of the distance (x) from the crack tip. Once the slip profile is known, the energy dissipation per unit extension of crack area can be estimated from eq 30 in the following form:

$$G − W = kV^n \int_0^\infty \left(\frac{\mathrm{d}u}{\mathrm{d}x}\right)^{1+n} \mathrm{d}x \tag{36}$$

Equations 35 and 36 have been verified recently in a model experiment,[72] in which a thin elastomeric silicone ribbon was peeled from a low energy surface produced by grafting PDMS chains to a glass slide. Fracture energies estimated ($1−10$ J/m²) for this system were considerably higher than the thermodynamic work of adhesion (~ 0.05 J/m²), but the results agreed well with the estimates based on eq 36. These studies provided definitive evidence that the energy dissipation due to frictional sliding can play an important role in the fracture of asymmetric interfaces.

10. Summary

The main issues addressed in this article are the roles of the reversible and irreversible interfacial processes in adhesion, friction, and fracture. Various examples, ranging from molecular weight and rate-dependent fracture energy to frictional sliding, portray the picture that interfacial processes, in general, are irreversible. The activated rate theory of Eyring, as extended by various authors including Schallamach and Evans et al., provides a theoretical framework with which to estimate the energy dissipation in fracture and the frictional sliding of elastomeric interfaces. Some of the important findings of this research are summarized below.

First, we discussed the well-known Lake−Thomas effect, which states that energy to fracture an elastomeric interface is amplified due to the stretching and relaxation of polymer chains. Examination of the Lake−Thomas model reveals that the elastic energy dissipation in the polymer chain is coupled to a "zero-temperature" mode of bond fracture at the interface. The idea is somewhat similar to the Gent−Schultz model of viscoelastic fracture. These models often convey the notion that the irreversibility manifests only in the bulk, whereas the interface behaves reversibly. The kinetic theory of fracture, however, suggests that coupling between bulk dissipation and interfacial separation depends on the relative relaxation times of the interfacial and bulk processes. The corollary of the above statement is that no energy dissipation occurs in the bulk of an adhesive if the interface behaves reversibly. As a consequence, we need to look deeper into the relaxation processes at the interface in order to develop a comprehensive theory of viscoelastic fracture rather than focusing only on such parameters as "surface free energy" and "thermodynamic work of

Feature Article

J. Phys. Chem. B, Vol. 104, No. 17, 2000 **4029**

adhesion". How the bulk irreversible processes are coupled to the interfacial kinetic process is clearly the subject of further research.

Second, we used the activated rate theory to re-examine the frictional sliding behavior of elastomeric polymers on low energy surfaces. Here the interface can be modeled as composed of elastic springs, the ends of which undergo random walks by hopping from one potential well to next. The collective behavior of the springs can be described by solving a dynamic probability equation. The basis of the idea is that an external force biases the random walk, causing a net relative motion of the two surfaces. The process requires irrecoverable external work. The method, however, does not elucidate the modes of energy dissipation arising from the transition of the polymer chain from one metastable state to the next. The analysis, nonetheless, brings forth several points regarding adhesion and friction to light. First, while a polymer chain segment overcomes a single potential well during fracture, multiple potential wells need to be overcome during frictional sliding. This process effectively increases the residence time of a polymer chain in frictional sliding. Similar issues have been raised previously by other investigators working in the field of polymer adsorption and diffusion on a solid surface. Second, since the relaxation time varies exponentially with the depth of surface potential well, the relationship between adhesion and friction is nonlinear, at least, at low sliding velocities. Detailed understanding of the relationship between adhesion and fracture is expected to emerge from additional systematic studies, in which not only the rate but also the temperature could be varied.

References and Notes

(1) Griffith, A. A. *Philos. Trans. R. Soc. London* **1920**, *221A*, 163.

(2) Gent, A. N.; Schultz, J. *J. Adhes.* **1972**, *3*, 281.

(3) Andrews, E. H.; Kinloch, A. J. *Proc. R. Soc. London* **1973**, *A332*, 385.

(4) Greenwood, J. A.; Johnson, K. L. *Philos. Mag.* **1981**, *A43* (3), 697.

(5) Huh, C.; Scriven, L. E. *J. Colloid Interface Sci.* **1971**, *35* (1), 85.

(6) Cox, R. G. *J. Fluid Mech.* **1986**, *168*, 169.

(7) de Gennes, P. G.; Hua, X.; Levinson, P. *J. Fluid Mech.* **1990**, *212*, 55.

(8) Blake, T. D.; Haynes, J. M. *J. Colloid Interface Sci.* **1969**, *30*, 421.

(9) Chaudhury, M. K. *Mater. Sci. Eng.* **1996** *19*, 30.

(10) Owen, M. J. *J. Coatings Technol.* **1981**, *53*, 49.

(11) Tobolsky, A. V. In *Properties and Structures of Polymers*; John Wiley & Sons: New York, 1960; p 67.

(12) Chaudhury, M. K.; Whitesides, G. M. *Langmuir* **1991**, *7*, 1013.

(13) Chaudhury, M. K.; Whitesides, G. M. *Science* **1992**, *255*, 1230; Chaudhury, M. K. *J. Adhes. Sci. Technol.* **1993**, *7*, 669.

(14) Johnson, K. L.; Kendall, K.; Roberts, A. D. *Proc. R. Soc. London* **1971**, *A324*, 301.

(15) Roberts, A. D.; Tabor, D. *Proc. R. Soc. London* **1971**, *A325*, 323.

(16) Dupre, A. *Theorie Mechanique de la Chaleur*; Gauthier-Villars: Paris, *1869*; p 369.

(17) Kendall, K. J. *J. Phys. D: Appl. Phys.* **1975**, *8*, 1449.

(18) Maugis, D.; Barquins, M. *Adhesion and Adsorption of Polymers: Polymer Science and Technology*; Lee, L. H., Ed.; Plenum: New York, 1980; Vol. 12A, p 203; Barquins, M.; Courtel, R. *Wear* **1975**, *32*, 133.

(19) Mangipudi, V. S.; Tirrel, M. *Rubber Chem. Technol.* **1998**, *71*, 407. This is a good review of the recent developments of the SFA (surface force apparatus) based adhesion studies.

(20) Roberts, A. D. *Rubber Chem. Technol.* **1979**, *52*, 23.

(21) Kendall, K. *Wear* **1975**, *33*, 351.

(22) Charmet, J.; Verjus, C.; Barquins, M. *J. Adhes.* **1996**, *57*, 5.

(23) Barquins, M. *J. Nat. Rubber Res.* **1990**, *5*, 199.

(24) She, H.; Malotky, D.; Chaudhury, M. K. *Langmuir* **1998**, *14*, 3090.

(25) She, H.; Chaudhury, M. K. *Langmuir* **2000**, *16*, 622.

(26) Maugis, D.; Barquins, M. *J. Phys. Lett.* **1981**, *L95*, 42.

(27) Maugis, D.; Barquins, M. *J. Adhes.* **1981**, *13*, 53.

(28) Kendall, K. J. *J. Adhes.* **1973**, *5*, 179.

(29) Shanahan, M. E. R.; Michel, J. *Int. J. Adhes.* **1991**, *11*, 170.

(30) See also Perutz, S.; Kramer, E. J.; Baney, J.; Hui, C.-Y. *Macromolecules* **1997**, *30*, 7964, and references therein.

(31) Lake, G. J.; Thomas, A. G. *Proc. R. Soc. London* **1967**, *A300*, 108.

(32) Barenblatt, G. I. *Adv. Appl. Mech.* **1962**, *7*, 55.

(33) Rice, J. R. *Appl. Mech. Trans. ASME* **1968**, *90*, 379.

(34) Some additional effects arise from the change of the surface energy of a polymer chain during stretching, as discussed in: Raphael, E.; de Gennes, P. G. *J. Phys. Chem.* **1992**, *96*, 4002.

(35) Bell, G. I. *Science* **1978**, *200*, 618.

(36) Brunk, D. K.; Goetz, D. J.; Hammer, D. A. *Biophys. J.* **1996**, *71*, 2902; Chang, K. C.; Hammer, D. A. *Langmuir* **1996**, *12*, 2271; Hammer, D. A.; Apte, S. M. *Biophys. J.* **1992**, *62*, 35.

(37) Evans, E.; Ritchie, K. *Biophys. J.* **1997**, *72*, 1541, and references therein.

(38) Merkel, R.; Nassoy, P.; Leung, A.; Ritchie, K.; Evans, E. *Nature* **1999**, *397*, 50.

(39) Schallamach, A. *Wear* **1963**, *6*, 375.

(40) Zhurkov, S. N.; Narzullayev, B. N. *Zh. Tekh. Fiz.* **1953**, *23*, 1677.

(41) Zhurkov, S. N.; Tomashevkii, E. Y. *Zh. Tekh. Fiz.* **1955**, *25*, 66.

(42) Zhurkov, S. N.; Sanfirova, T. P.; *Dokl. Akad. Nauk SSSR* **1955**, *101*, 237.

(43) Bueche, F. *J. Appl. Phys.* **1955**, *26*, 1133.

(44) Bueche, F. *J. Appl. Phys.* **1957**, *28*, 784.

(45) Bueche, F. *J. Appl. Phys.* **1958**, *29*, 1231.

(46) Kausch, H. H. *Kolloid-Zeitschrift und Zeitschrift fur Polymer* **1970**, *236*, 48.

(47) Kausch, H. H. *J. Polymer Sci.* **1971**, *C32 (Polymer Symposium)*, 1.

(48) Kausch, H. H. *Polymer Fracture*, Vol. 2; Springer-Verlag: New York 1978.

(49) Tobolsky, A.; Eyring, H. *J. Chem. Phys.* **1943**, *11*, 125.

(50) Chaudhury, M. K. *J. Phys. Chem. B* **1999**, *103* (31), 6562.

(51) Quantitative interpretation of the results obtained with these H-bonding systems suffers from the complication that the experimentally (Figure 5) observed relationship ($G \propto M^{1.5}$) between the fracture energy and molecular weight deviates from that predicted ($G \propto M^{1/2}$) by eq 17. The origin of this departure may be due to the interfacial entanglement of polymer chains, which distributes the applied force to multiple attachment sites on the surface. Since each chain makes approximately $\sqrt{n}$ number of contacts with the surface, the force on a chain is distributed to approximately $\sqrt{n}$ number of surface sites. If f is the force needed to desorb a polymer chain from a single site, then the total fracture energy is: $G_{el} = \Sigma_o/2k_s$ ($\sqrt{n}f)^2$, which predicts that G_{el} varies with molecular weight as $G_{el} \propto M^{1.5}$. Here, we have refrained from these higher corrections. See also Choi et al. (Choi, G. Y.; Zurawsky, W. P.; Ulman, A. *Langmuir* **1999**, *15*, 8447) and the references cited therein for further discussions on the effect of molecular weight on adhesion hysteresis.

(52) Kramers, H. A. *Physica* **1940**, *VII* (4), 284.

(53) Hanggi, P.; Talkner, P.; Borkovec, M. *Rev. Mod. Phys.* **1990**, *62* (2), 251.

(54) Previously, She et al.[24] found that the majority of these detachment forces cluster around 50−100 pN range. Subsequently, we noted that when a SiO$_2$ tip is used immediately after plasma oxidation, forces as high as 2−2.5 nN could be measured. Some of the pioneering studies of chain elasticity using AFM can be found in the following references: Senden, T. J.; di Meglio, J. M.; Auroy, P. *Eur. Phys. J. B* **1998**, *3*, 211; Reif, M.; Oesterhelt, F.; Heymann, B.; Gaub, H. E. *Science* **1997**, *275*, 1295; Ortiz, C.; Hadziioannou, G. *Macromolecules* **1999**, *32*, 780; Bemis, J. E.; Akhremitchev, B. B.; Walker, G. C. *Langmuir* **1999**, *15*, 2799.

(55) Marko, J. F.; Siggia, E. D. *Macromolecules* **1995**, *28*, 8759.

(56) Smoluchowski, M. V. *Ann. Phys. (Leipzig)* **1906**, *21*, 756.

(57) Owen, M. J.; Jones, D. Silicone Release Coatings. In *Polymer Materials Encyclopedia*; Salamone, J. C., Ed.; CRC Press LLC: Boca Raton, FL, 1996; p 7688.

(58) *Release Agents*. In *Encyclopedia of Polymer Science and Engineering*, 2nd ed.; Wiley-Interscience: New York, 1988; Vol. 14, p 411.

(59) Bey, A. E. *Adhesives Age* **1972**, *15* (10), 29.

(60) Ahn, D.; Shull, K. R. *Langmuir* **1998**, *14*, 3646; *Langmuir* **1998**, *14*, 3637; Shull, K. R.; Crosby, A. J. *J. Eng. Mater. Technol.* **1997**, *119*, 211.

(61) *Fundamentals of Friction: Macroscopic and Microscopic Processes*; Singer, I. L., Pollock, H. M., Eds.; Kluwer Academic Press: Boston, 1992.

(62) Gittus, J. H. *Philos. Mag.* **1975**, *32*, 317.

(63) Chaudhury, M. K. Current Opinion in *J. Colloid Interface Sci.* **1997**, *2*, 65.

(64) Johnson, K. L. *Proc. R. Soc. London* **1997**, *A453*, 163.

(65) Hurtado, J. A.; Kim, K.-S. *Proc. R. Soc. London* **1999**, *455*, 3363.

(66) Hurtado, J. A.; Kim, K.-S. *Proc. R. Soc. London* **1999**, *455*, 3385.

(67) Grosch, K. A. *Proc. R. Soc. London* **1963**, *A274*, 21.

(68) Subbotin, A.; Semenov, A.; Manias, E.; Hadziioannou, G. *Macromolecules* **1995**, *28*, 1511.

(69) Subbotin, A.; Semenov, A.; Hadziioannou, G.; ten Brinke, G. *Macromolecules* **1996**, *29* (4), 1296.

(70) Brown, H. R. *Science* **1994**, *263*, 1411.

(71) Chaudhury, M. K.; Owen, M. J. *Langmuir* **1993**, *9*, 29.

(72) Newby, B−m. Z.; Chaudhury, M. K. *Langmuir* **1998**, *14*, 4865.

(73) Chandrasekhar, S. *Rev. of Mod. Phys.* **1943**, *15* (1), 1.

(74) Reiter, G.; Casoli, A. Personal communication.

(75) Léger, L.; Hervet, H.; Durliat, E. *J. Phys.: Condens. Matter* **1997**, *9*, 7719.

(76) Galt, J.; Maxwell, B. *Mod. Plast.* **1964**, *42* (12), 115.

(77) de Gennes, P. G. *C. R. Acad. Sci. Paris* **1979**, *B288*, 219.

(78) Kraynik, A. M.; Schowalter, W. R. *J. Rheol.* **1981**, *25* (1), 95.

(79) Burton, R. H.; Folkes, M. J.; Narh, K. A.; Keller, A. *J. Mater. Sci.* **1983**, *18*, 315.

(80) Ramamurthy, A. V. *J. Rheol.* **1986**, *30* (2), 337.

(81) Hill, D. A.; Hasegawa, T.; Denn, M. M. *J. Rheol.* **1990**, *34* (6), 891.

(82) Brochard, F.; de Gennes, P. G. *Langmuir* **1992**, *8*, 3033.

(83) Hatzikiriakos, S. G.; Dealy, J. M. *J. Rheol.* **1992**, *36* (4), 703.

(84) Inn, Y. W.; Wang, S. Q. *Phys. Rev. Lett.* **1996**, *76*, 467.

(85) Granick, S. *MRS Bull.* **1996**, *21*, 33.

(86) Newby, B−m. Z.; Chaudhury, M. K.; Brown, H. R. *Science* **1995**, *269*, 1407.

(87) Hutchinson, J. W.; Suo, Z. *Adv. Appl. Mech.* **1992**, *29*, 63.

(88) Newby, B−m. Z.; Chaudhury, M. K. *Langmuir* **1997**, *13*, 1805.